Calibration of wafer surface inspection systems using spherical silica nanoparticles

Thomas A. Germer,[1] **Christian Wolters,**[2] **and Don Brayton**[2]

[1]*National Institute of Standards and Technology (NIST), Gaithersburg, Maryland, 20899*
[2]*KLA-Tencor Corporation, One Technology Drive, Milpitas, California 95035*

thomas.germer@nist.gov

Abstract: Silica nanospheres with diameters ranging from 60 nm to 269 nm are investigated as an alternative to polystyrene spheres for calibrating laser-scattering-based wafer surface inspection systems, since they are less susceptible to changes upon ultraviolet exposure. Polystyrene and silica spheres were classified by differential mobility analysis before being deposited onto bare silicon wafers, and scattered signals were measured by two commercial tools using 488 nm and 355 nm laser light. The instrument signals were modeled by integrating a theoretically-determined differential cross section over the collection geometry of each tool, and the predicted signals were compared to the measured signals. The resulting calibrations, whether performed using the polystyrene spheres, the silica spheres, or both, were found to be equivalent and to meet industry requirements, provided the index of refraction of the silica spheres was allowed to be a floating parameter. The indices were found to be 1.413 and 1.421 at 488 nm and 355 nm, respectively, consistent with a void fraction of 11.4%.

OCIS codes: (120.4800) Optical standards and testing; (290.5850) Scattering, particles; (120.4630) Optical inspection; (290.3030) Index measurements.

References and links

1. E. Marx and G. W. Mulholland, "Size and refractive index determination of single polystyrene spheres," J. Res. Natl. Bur. Stand. **88**, 321–338 (1983).
2. G. W. Mulholland, A. W. Hartman, G. G. Hembree, E. Marx, and T. R. Lettieri, "Development of a one-micrometer-diameter particle size standard reference material," J. Res. Natl. Bur. Stand. **90**, 3–26 (1985).
3. G. W. Mulholland, N. P. Bryner, and C. Croarkin, "Measurement of the 100 nm NIST SRM 1963 by differential mobility analysis," Aerosol Sci. and Technol. **31**, 39–55 (1999).
4. SEMI Standard M53, "Practice for Calibrating Scanning Surface Inspection Systems using Certified Depositions of Monodisperse Polystyrene Latex Spheres on Unpatterned Semiconductor Wafer Surfaces," available from Semiconductor Equipment and Materials International, 3081 Zanker Road, San Jose, CA 95134, http://www.semi.org.
5. P. A. Bobbert and J. Vlieger, "Light scattering by a sphere on a substrate," Physica **137A**, 209–242 (1986).
6. P. A. Bobbert, J. Vlieger, and R. Greef, "Light reflection from a substrate sparsely seeded with spheres–comparison with an ellipsometric experiment," Physica **137A**, 243–257 (1986).
7. T. A. Germer, "Modeled Integrated Scatter Tool (MIST)," available from http://physics.nist.gov/scatmech.
8. T. A. Germer, "SCATMECH: Polarized Light Scattering C++ Class Library," available from http://physics.nist.gov/scatmech.
9. J. H Kim, G. W. Mulholland, S. H. Ehrman, and T. A. Germer, "Polarized light scattering from dielectric and metallic spheres on silicon wafers," Appl. Opt. **41**, 5405–5412 (2002).

#92609 - $15.00 USD Received 11 Feb 2008; revised 7 Mar 2008; accepted 9 Mar 2008; published 20 Mar 2008

10. J. H. Kim, S. H. Ehrman, G. W. Mulholland, and T. A. Germer, "Polarized light scattering by dielectric and metallic spheres on oxidized silicon surfaces," Appl. Opt. **43**, 585–591 (2004).
11. J. H. Kim, S. H. Ehrman, and T. A. Germer, "Influence of particle oxide coating on light scattering by submicron metal particles on silicon wafers," Appl. Phys. Lett. **84**, 1278–1280 (2004).
12. C. M. Herzinger, B. Johs, W. A. McGahan, J. A. Woollam, and W. Paulson, "Ellipsometric determination of optical constants for silicon and thermally grown silicon dioxide via a multi-sample, multi-wavelength, multi-angle investigation," J. Appl. Phys. **83** , 3323–3336 (1998).
13. *Styrene, Its Polymers, Copolymers, and Derivatives*, R. H. Boundy and R. F. Boyer, eds., (Reinhold, New York, 1952).
14. E. D. Palik, *Handbook of Optical Constants of Solids*, (Academic, San Diego, 1985).
15. E. O. Knutson and K. T. Whitby, "Aerosol classification by electric mobility: apparatus, theory, and applications," J. Aerosol Sci. **6**, 443–451 (1975).
16. P. D. Kinney, D. Y. H. Pui, G. W. Mulholland, and N. P. Bryner, "Use of the electrostatic classification method to size 0.1 μm SRM particles–a feasibility study," J. Res. Natl. Inst. Stand. Technol. **96**, 147–176 (1991).
17. Certain commercial equipment, instruments, or materials are identified in this paper in order to specify the experimental procedure adequately. Such identification is not intended to imply recommendation or endorsement by the National Institute of Standards and Technology, nor is it intended to imply that the materials or equipment identified are necessarily the best available for the purpose.
18. SEMI Standard M52, "Guide for Specifying Scanning Surface Inspection Systems for Silicon Wafers for the 130 nm, 90 nm, 65 nm, and 45 nm Technology Generations," available from Semiconductor Equipment and Materials International, 3081 Zanker Road, San Jose, CA 95134, http://www.semi.org.
19. H. G. Tompkins *A User's Guide to Ellipsometry*, (Academic, San Diego, 1993).
20. The uncertainties quoted in this article were obtained by estimating the standard uncertainty u for the measurement and multiplying by a coverage factor of $k = 2$. These values correspond to a confidence level of 95%.

1. Introduction

Polystyrene (PS) spheres are often used as particle size reference standards due to their ideal shape, homogeneity, and narrow size distribution.[1, 2, 3] These particles are provided as a colloidal solution. In the semiconductor industry, they are aerosolized, classified to narrow their distribution further, deposited onto silicon wafers, and used for calibrating wafer surface inspection systems. However, it has been found that under ultraviolet illumination, increasingly used by these systems, the polystyrene spheres degrade. Recently, spherical silica particles have become available that might provide an ultraviolet-stable alternative to PS spheres. In order for silica particles to be accepted as a new reference standard, there must be sound scientific and technological evidence that the transition will not result in a loss of accuracy or a change in scale.

A standard calibration procedure was developed to improve the calibration of wafer inspection systems.[4] This procedure calls for measuring the signals from a set of PS particle sizes and comparing those signals with those calculated by theoretically modeling the response of the inspection system. The procedure provides the calibration that enables the instrument to deduce scattering cross section, integrated over the collection geometry of the system. Once the system has been calibrated in this manner, signals can then be interpreted in terms of an effective PS sphere diameter that would yield the same integrated cross section.

In this article, we investigate whether silica spheres could substitute for PS spheres for calibrating light-scattering-based systems. These spheres are significantly more stable under ultraviolet irradiation. However, their size distributions are generally too broad to be used as size standards straight out of the bottle. Nonetheless, they can be size-classified, using polystyrene sphere standards to calibrate the classifier, before being deposited onto wafers. We fabricated two wafers, one with depositions of PS spheres and one with depositions of silica spheres having identical sizes. The resulting calibration was then found to be comparable to that obtained with PS spheres, provided we allow the index of refraction of the particles to vary.

We describe the theoretical modeling in Sec 2. The deposition of PS and silica particles on test wafers is described in Sec. 3. In Sec. 4, we describe the instruments that were used to

#92609 - $15.00 USD Received 11 Feb 2008; revised 7 Mar 2008; accepted 9 Mar 2008; published 20 Mar 2008

measure the light scattering from the particles. In Sec. 5, we analyze the light scattering signals that were obtained from the particles, and evaluate the consistency of calibrations performed with the two different particle materials. The results are discussed in Sec. 6, and in Sec. 7 we make some conclusions.

2. Scattering theory

The theory of Bobbert and Vlieger[5, 6] describes the solution to the scattering of an electromagnetic wave incident upon a homogeneous sphere above a surface. The theory can be straightforwardly extended to include coatings on the surface and the sphere, provided the sphere does not embed itself into the surface. We use computer code developed by one of the authors[7, 8] to evaluate the differential scattering cross section $\sigma_\Omega(\theta,\phi,D)$, where θ is the polar scattering angle, ϕ is an azimuthal scattering angle, and D is the diameter of the sphere. The differential scattering cross section is also a function of the incident angle, polarization, wavelength, the optical properties of the substrate and the particle, and the thicknesses and optical properties of any coatings on either the substrate or the particle. The computer code has been thoroughly tested using a variety of model systems.[9, 10, 11] In all calculations provided here, we included the effects of a 1.6 nm native oxide coating on the silicon substrate. The integrated cross section as a function of particle diameter is given by

$$\Sigma(D) = \int \mathrm{d}\theta\, \mathrm{d}\phi\, \sin\theta\, \sigma_\Omega(\theta,\phi,D), \tag{1}$$

where the integral is over the set of directions (θ and ϕ) collected by the collection optics of the system. We use $\Sigma_{\mathrm{PS}}(D)$ and $\Sigma_{\mathrm{silica}}(D)$ to denote the integrated cross section using optical properties for PS and silica particles, respectively. The optical constants that we used for the materials are given in Table 1.

Table 1. Optical constants used for the modeling.

	488 nm		355 nm		
Material	n	k	n	k	Ref.
silicon	4.368	0.040	5.712	2.962	[12]
native oxide	1.739	0	1.749	0	[12]
PS	1.605	0	1.650	0	[13]
bulk silica	1.465	0	1.478	0	[14]

3. Particle deposition

Spherical polystyrene and silica particles were classified by a differential mobility analyzer[15, 16] (DMA) before being deposited onto silicon wafers. The initial particle sizes were approximately matched, and the settings for the DMA were identical for each particle size. Therefore, identical sizes of the two materials were deposited. The flow conditions of the DMA were such that the full-width at half-maximum (FWHM) of the DMA passband was approximately 5% of the central pass diameter. Three of the PS particles were NIST Standard Reference Materials $^{\mathrm{TM}}$ (SRM), and the DMA was calibrated to match the certified values of one of these references. Approximately 2000 particles were deposited of each size. Table 2 summarizes the sizes used in this study. The DMA setting has an arbitrary scale which is linearly related to the particle diameter. The corrected diameter is determined by multiplying the DMA setting by a constant so that the 101.8 nm particle size matches that certified.

#92609 - $15.00 USD Received 11 Feb 2008; revised 7 Mar 2008; accepted 9 Mar 2008; published 20 Mar 2008

Table 2. Particle diameters deposited on wafers.

Nom. Diameter [nm]	DMA Setting [a.u.]	Corrected Diameter [nm]
60.4 ± 0.6*	57.0	59.8
73	69.7	73.1
101.8 ± 1.1*	97.0	101.8
126	120.3	126.3
155	148.0	155.3
204	194.8	204.4
269 ± 4*	256.0	268.7

*The PS particles were NIST SRM^{TM}.

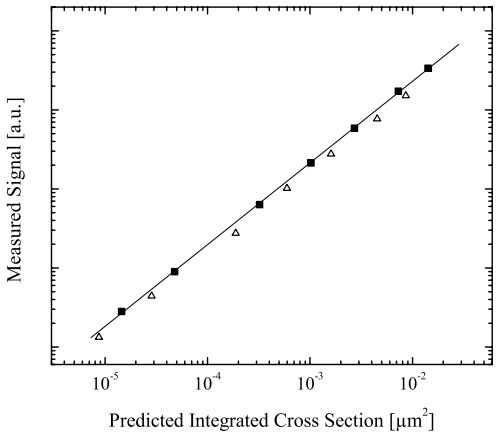

Fig. 1. The measured signal as a function of predicted signal measured for PS spheres (solid squares) and silica spheres (open triangles). The index assumed for the silica spheres is that of bulk silica. The straight line is a least-squares best fit of a straight line to the PS sphere data.

4. Scattering measurements

Scattering measurements were performed on two models of wafer scanners, the KLA-Tencor SP-1 and the KLA-Tencor SP-2.[17] The SP-1 operates at 488 nm, while the SP-2 operates at 355 nm. Both instruments use p-polarized light incident at an oblique angle and collect a large annulus of scattering directions centered on the surface normal (the "wide" channel). Both instruments scan the wafer under the laser beam and extract a signal for light scattering events, corresponding to individual particles on the wafer. The locations of each event is recorded along with its respective signal. Histograms of the particle signals are then generated and the peak signal noted for each deposition.

5. Results

The data were analyzed in a manner similar to that prescribed by SEMI Standard M53.[4] Figure 1 shows the signals $S(D_i)$ from the PS spheres measured on the 488 nm tool as a function of that predicted by the model calculations, $\Sigma_{\text{silica}}(D_i)$. Note that the vertical scale is not labeled, since it represents an arbitrary unit. The results lie along a straight line on a log-log graph, with a slope of 1.034 ± 0.012 [20], thus defining the gain-nonlinearity function $g(\Sigma)$ between

#92609 - $15.00 USD Received 11 Feb 2008; revised 7 Mar 2008; accepted 9 Mar 2008; published 20 Mar 2008

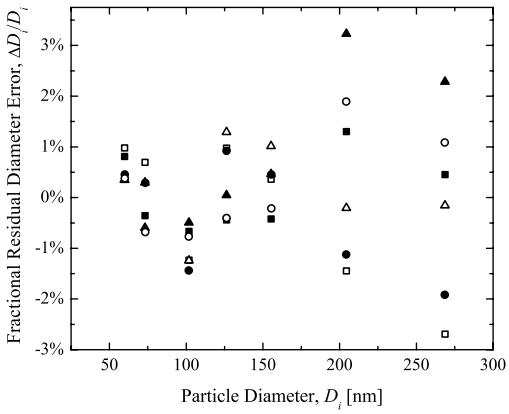

Fig. 2. The residual fractional diameter error determined from calibrations at 488 nm. The closed symbols and open symbols represent the fractional residual error for PS and silica particles, respectively. The squares, triangles, and circles represent the results when the system was calibrated with PS, silica, and both particles, respectively.

measured signal and predicted signal, so that $S(D) = g[\Sigma(D)]$. The residuals of the fit, expressed in terms of fraction of diameter, calculated from

$$\frac{\Delta D_i}{D_i} = \frac{\Sigma_{\text{silica}}^{-1}\{g^{-1}[S(D_i)]\} - D_i}{D_i} \tag{2}$$

are shown in Fig. 2, where $g^{-1}(S)$ is the inverse of $g(\Sigma)$, and $\Sigma_{\text{silica}}^{-1}(x)$ is the inverse of $\Sigma_{\text{silica}}(D)$. The root mean square (rms) deviation of the residual is $\sigma = 0.7\%$. According to [4], the expanded PS sphere sizing uncertainty, representing the 95% confidence limit, is given by

$$U = 2[(\sigma + u_{\text{dep}})/(N - M)]^{1/2}, \tag{3}$$

where u_{dep} is the standard uncertainty of the deposition diameter, $N = 7$ is the number of sphere sizes, and $M = 2$ is the number of degrees of freedom of the fit. If we let $u_{\text{dep}} = 1.5\%$ be the maximum recommended value for the deposition uncertainty, assumed to be the specification required for the deposition systems, the PS sphere sizing uncertainty is $U = 1.5\%$. Industry standards require that this value be less than 2%.[18] Table 3 presents the rms of the residuals, σ, and the expanded uncertainty U. Once the inspection system is calibrated, as described above, the reported PS-equivalent diameter of a light scattering event yielding signal S is

$$D = \Sigma_{\text{PS}}^{-1}[g^{-1}(S)]. \tag{4}$$

Figure 3 shows the results of applying Eq. 4 to the 488 nm silica data. The silica particles, because their index is less than that of PS, appear smaller than identically-sized PS spheres. The ratio of the PS-equivalent diameter to the actual diameter is not a constant. Furthermore, that ratio will depend upon the optical geometry and wavelength, so that there is no universal relationship between PS-equivalent diameter and actual diameter.

When we performed the analysis above to the silica sphere data using literature values for the index of refraction of silica, we find that the results do not lie on the same straight line seen for the PS spheres (see Fig. 1). Presumably, the index of refraction of the silica spheres differ from that of bulk silica due to porosity. Lowering the index of refraction will move the silica data

#92609 - $15.00 USD Received 11 Feb 2008; revised 7 Mar 2008; accepted 9 Mar 2008; published 20 Mar 2008

Table 3. Summary of the calibration results.

	SP-1: 488 nm		
	PS Calibration	Silica Calibration	Joint Calibration
PS Sizing (1σ)	0.7%	1.5%	1.0%
Silica Sizing (1σ)	1.4%	0.8%	
PS Sizing (U)	1.5%	1.6%	1.0%
Silica Sizing (U)	1.5%	1.5%	
	SP-2: 355 nm		
	PS Calibration	Silica Calibration	Joint Calibration
PS Sizing (1σ)	0.6%	1.0%	1.1%
Silica Sizing (1σ)	1.5%	1.5%	
PS Sizing (U)	1.4%	1.4%	1.1%
Silica Sizing (U)	1.6%	1.9%	

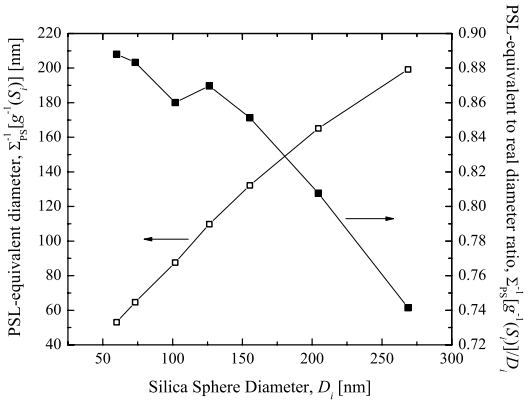

Fig. 3. Results of applying the calibration to the silica spheres at 488 nm: (open symbols, left scale) the PS-equivalent diameter of the silica particles and (solid symbols, right scale) the ratio of that diameter to the actual diameter.

in Fig. 1 to the left. By varying the index of refraction used during the modeling of $\Sigma_{\text{silica}}(D)$, we find that the mean square residual between the silica signals and $g[\Sigma(D)]$ (the straight line in Fig. 1) was minimized when we used the value of 1.413 ± 0.008 at 488 nm. This index is lower than the literature value for bulk silica (see Table 1) by 3.5%. The rms of the relative residual diameter was 0.8%, only slightly larger than that found for the PS calibration at this wavelength.

We also considered the cross-residuals obtained by the silica particles when the system was calibrated with PS particles, and vice versa. In this case, we use

$$D = \Sigma_j^{-1}[g_k^{-1}(S)], \tag{5}$$

where the subscript j indicates the particle material being measured, while subscript k indicates the particle material under which the system is calibrated. The results of the cross-residuals are included in Table 3. The values of the rms of the cross-residuals were always larger than those obtained from the calibration, because there are a different number of degrees of freedom for the cross-residuals than for the calibration residuals. When calculating the expanded particle size uncertainty U from the cross-residuals, we include the fact that the number of fitting parameters

#92609 - $15.00 USD Received 11 Feb 2008; revised 7 Mar 2008; accepted 9 Mar 2008; published 20 Mar 2008

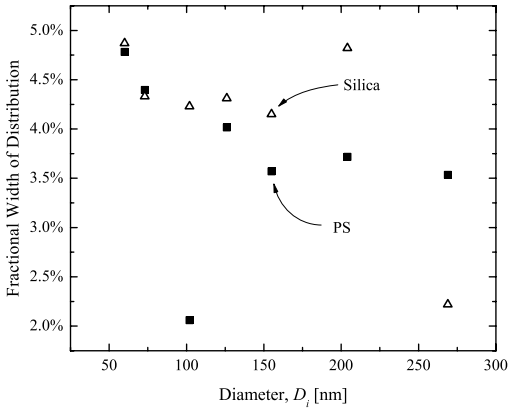

Fig. 4. The apparent FWHM of the size distribution of the (solid squares) PS and (open triangles) silica particles measured at 488 nm.

M is zero. When considering this fact, the expanded particle size uncertainty difference between the two particle types is insignificant.

Lastly, we considered the residuals obtained when we considered all of the particles, both PS and silica, during the calibration step. The residuals were found to be similar to those obtained with a single particle material, but the total expanded uncertainty was significantly less, because the number of data points M increased by a factor of two. One of the advantages of the calibration procedure is that an increase in the number of calibration particle sizes will improve the overall uncertainty in resulting measurements.

The widths of the distributions of the effective particle sizes deposited on the wafers were estimated by examining the histograms of the signals. The width of the signal on a logarithmic scale can be divided by the logarithmic derivative of the predicted signal for the respective material to yield the FWHM of the size distribution. Figure 4 shows the results of this analysis for the 488 nm data. All of the particle distributions have widths below the 5% band pass of the DMA. The actual distribution would be determined by the product of the source particle distribution and the DMA passband. The silica particles tend to have larger apparent widths, which would be expected from the wider distributions of the source particles. Non-spherical particles would be expected to increase the apparent width of the distributions. Since none of the particle sizes had an apparent width larger than the DMA pass band, we can rule out a significant contribution from non-spherical particles.

An identical analysis was performed using the SP-2 operating at 355 nm using the same particle depositions. The index of refraction for the particles was found to be 1.421 ± 0.008 at 355 nm. A summary of the residuals and resulting uncertainties is included in Table 3.

6. Discussion

The index of refraction can be considered in terms of effective medium theory. Maxwell-Garnett theory is appropriate for voids within a host material.[19] The effective index n_{eff} is related to the host index n_{h} and the void fraction x by

$$n_{\mathrm{eff}}^2 = \frac{n_{\mathrm{h}}^2(1-2n_{\mathrm{h}}^2(x-1)+2x)}{1-x+n_{\mathrm{h}}^2(x+2)}. \tag{6}$$

#92609 - $15.00 USD Received 11 Feb 2008; revised 7 Mar 2008; accepted 9 Mar 2008; published 20 Mar 2008

Eq. (6) can be solved for the void fraction

$$x = \frac{2n_{\mathrm{h}}^4 - 2n_{\mathrm{eff}}^2 n_{\mathrm{h}}^2 + n_{\mathrm{h}}^2 - n_{\mathrm{eff}}^2}{(n_{\mathrm{h}}^2 - 1)(2n_{\mathrm{h}}^2 + n_{\mathrm{eff}}^2)} \tag{7}$$

Using the data from the two wavelengths, we find that $x = 0.110 \pm 0.016$ at 488 nm and $x = 0.117 \pm 0.016$ at 355 nm. Thus, the two results are equivalent with one another, within the uncertainties of the measurements.

The finding that the calibrations performed with silica particles were equivalent to those obtained with PS particles suggest that all of the particle sizes had the same index of refraction. However, what needs to be determined is how universal that index is for silica nanospheres. All of the silica spheres were obtained from one source, and another manufacturer may employ methods that yield different indices of refraction. Any reference wafer containing silica sphere depositions should certify not only the diameters of the spheres, but also the index of refraction of those spheres. The method described in this article may be used to determine that index.

7. Conclusion

Two wafer inspection systems, operating at 488 nm and 355 nm, were each calibrated using PS spheres, silica spheres, and both simultaneously. It was found that all of the calibrations were consistent with one another, provided the index of refraction of the silica was allowed to vary. The indices determined at the two wavelengths were found to be consistent with one another within the Maxwell-Garnett theory.

#92609 - $15.00 USD Received 11 Feb 2008; revised 7 Mar 2008; accepted 9 Mar 2008; published 20 Mar 2008